



Shaking Table Test Design for the Self-Installation Platform of Offshore Converter Stations

Lihe Wang¹, Zhaorong Ma¹, Can Zheng¹, Zhiwei Niu^{2*}, Renfeng Zheng², Fangjie Li²

¹ China Energy Engineering Group Guangdong Electric Power Design Institute Co., Ltd., 510663 Guangzhou, China

² College of Water Conservancy and Hydropower Engineering, Hohai University, 210098 Nanjing, China

* Correspondence: Zhiwei Niu (nzw@hhu.edu.cn)

Received: 07-28-2025

Revised: 09-30-2025

Accepted: 10-08-2025

Citation: L. H. Wang, Z. R. Ma, C. Zheng, Z. W. Niu, R. F. Zheng, and F. J. Li, "Shaking table test design for the self-installation platform of offshore converter stations," *J. Civ. Hydraul. Eng.*, vol. 3, no. 4, pp. 188–199, 2025. <https://doi.org/10.56578/jche030402>.



© 2025 by the author(s). Licensee Acadlore Publishing Services Limited, Hong Kong. This article can be downloaded for free, and reused and quoted with a citation of the original published version, under the CC BY 4.0 license.

Abstract: Offshore converter stations are the core equipment for large-scale transmission of energy from distant offshore wind farms. When designing and constructing converter station platforms in high seismic intensity regions, their seismic performance must be considered. Numerical simulation and shaking table model testing are two important methods for studying the structural dynamic characteristics and seismic response. The effectiveness of numerical simulations for investigating the seismic response of offshore converter station platforms needs to be validated through shaking table model tests. Due to the limitations of the shaking table's surface area and load capacity, the prototype structure must be scaled down based on similarity theory. To meet the test requirements, acrylic and aluminum alloy are selected as model materials for the pile legs and platform body, respectively. In order to simplify the model for testing, the pile legs are designed using a bending stiffness equivalence method, while the upper platform is designed to satisfy mass similarity and sufficient stiffness. The dynamic characteristics of the foundation-pile-soil interaction are equivalently modeled using numerical simulations. After the model is constructed, dynamic characteristic tests are performed, and the results are compared with the numerical simulation analysis of the prototype structure. The results indicate that the selected model materials and simplified design are reasonable, providing a useful reference for shaking table tests of similar offshore platforms.

Keywords: Offshore converter station; Self-installation platform; Shaking table; Test design; Model similarity

1 Introduction

With the development of offshore wind power in China towards larger capacity, larger turbines, far-offshore, and deep-water areas [1], the large-scale transmission of electricity from distant offshore wind farms requires High Voltage Direct Current (HVDC) technology for efficient grid connection. Offshore converter stations are the key core equipment for offshore wind power DC transmission. The development of distant offshore wind farms requires the construction of offshore converter stations, which need to integrate the converter equipment into specialized offshore platforms. Currently, the main types of offshore electrical platforms are jacket type, semi-submersible type, and self-installing type [1]. The installation methods of the upper blocks of offshore platforms can be classified into lifting method, self-installation method, and floating support method. Self-installation refers to the method where the platform does not rely on external resources or equipment and is installed in the designated sea area by its own equipment capabilities [2]. The construction of offshore converter stations using self-installing platforms adopts the self-installation method. A self-installing converter station platform consists of the platform body, pile legs, and lifting devices, relying on its pile legs and lifting devices to raise the platform body to meet operational requirements. Although jacket platforms are widely adopted due to their simple structural design, relatively low cost, and other advantages [3], self-installing platforms have the following prominent advantages over jacket platforms: self-installing platforms use modern shipbuilding modes, significantly shortening the construction period and being less affected by the marine environment [4]; self-elevating platforms achieve self-installation through hydraulic lifting systems without relying on large floating cranes or complex marine engineering equipment, reducing construction difficulty and dependency on external resources [2]. Using self-installing platforms to build offshore converter stations can take advantage of the limited offshore construction window to complete the construction quickly, improving project

efficiency. However, the self-installing platform of the converter station is large, structurally flexible, and costly, and the offshore waters in China and its neighboring regions are located at the junction of several tectonic plates, making the marine area subject to frequent seismic activities [5]. Therefore, it is necessary to conduct seismic response analysis and research of offshore converter stations for reasonable seismic design to ensure the safety of offshore wind power equipment and its supporting structures, while avoiding a significant increase in the design cost of the supporting structures.

Researching the dynamic characteristics and seismic response of structures can be done using numerical simulations and shaking table model tests. In terms of numerical simulations, Shao et al. [6] used finite element method for numerical simulation to analyze the seismic resilience of the nonlinear jacket platform structure and found that considering structural nonlinearity could significantly reduce the pile foundation wall thickness, thus reducing costs. Jin et al. [7] established a numerical model of jacket platforms under the combined effect of earthquakes and typhoons and conducted time history analysis. The results showed that under the coupled effect of earthquake and typhoon, the safety performance of the platform significantly decreased, and the maximum stress in most working conditions occurred in the same component, suggesting that structural weak parts should be appropriately reinforced during design. Li [8] used LS-DYNA's explicit dynamic algorithm to analyze the dynamic response of the jacket platform under earthquake intensities of 7, 8, and 9 degrees and found that the "amplification" effect of seismic response was more obvious for components located higher in the structure. Wu et al. [9] discussed the influence of response spectrum method and time history analysis method on the seismic performance analysis of jacket platforms, concluding that the response spectrum method is suitable for the elastic seismic stage, while the time history method is appropriate for the elastoplastic seismic stage. Ghazi et al. [10] studied the dynamic response of self-elevating platforms under various environmental load couplings at different heights, finding that the dynamic response of the structure was significantly affected by platform height. Sun et al. [11] used vector-based finite element method to analyze the dynamic response of converter station platforms with jacket foundations and found that peak responses increased almost linearly with the ground peak acceleration, and observed that the vertical acceleration of the valve hall deck was significantly greater than that of other structures.

Regarding shaking table model tests, Zhao et al. [12] designed a jacket platform model with a geometric scale of 1:60 based on hydro-elastic similarity laws for shaking table tests. The tests showed that under seismic excitation, the acceleration response distribution along the elevation of the platform structure exhibited a whip effect, first decreasing and then increasing. Xie et al. [13] made a self-elevating platform model with a geometric scale of 1:150 for shaking table tests and found that low-frequency seismic waves were more harmful to offshore platforms, while high-frequency seismic waves increased the risk of shallow soil liquefaction. Chai et al. [14] studied the dynamic response of self-elevating platforms on sandy seabeds under horizontal cyclic loading and found that the effect of horizontal cyclic loading on sandy seabed foundations could not be ignored, and increasing the pile penetration depth could improve the horizontal bearing capacity of the foundation. Liu [15] used shaking table tests to study the vibration control effect of collision-tuned mass dampers (PTMD) on self-elevating platforms, concluding that PTMD has better control effects than TMD. Lou et al. [16] conducted shaking table tests on offshore electrical platforms of jacket type and found that the dynamic response of the structure was closely related to the structural dynamic characteristics and the spectral characteristics of the exciting seismic waves. He and Pan [17] conducted underwater shaking table tests on offshore wind turbines, concluding that the effect of hydrodynamic pressure on the structural acceleration response could either amplify or reduce, depending on the inherent dynamic characteristics of the structure and the spectral characteristics of the seismic excitation. Ko and Li [18] conducted shaking table tests on jacket foundations of offshore wind turbine generators on liquefiable foundations, finding that after soil liquefaction, the ground response was significantly reduced, and there were differences in acceleration responses between the soil and jacket foundation. Additionally, after liquefaction, the bending moment response significantly decreased due to the low dynamic soil pressure. Huang et al. [19] used model tests and numerical simulations to analyze the impact of offshore and onshore earthquakes on the dynamic response of jacket platforms, finding that low-frequency energy dominated the offshore seismic waves, and the natural period of offshore structures was longer. They concluded that conducting seismic analysis of marine platforms based on land earthquakes might overestimate their seismic resistance. Liu et al. [20] considered soil-water-structure interaction and established a jacket platform model with a geometric scale of 1:20 for shaking table tests, discovering that soil helped reduce the peak acceleration and maximum inter-story displacement ratio of the jacket marine platform, while hydrodynamic pressure would change the acceleration Fourier spectrum of the jacket marine foundation platform.

Due to the high accuracy, strong adaptability, and cost-effectiveness of numerical simulation methods, most seismic response analyses use numerical simulation methods. Most existing research focuses on jacket platforms, with less attention paid to self-installing platforms. The shell-type pile legs of self-installing platforms are significantly different from the piles of jacket platforms; self-installing platform pile legs have larger diameters and are subject to hydrodynamic pressure on both their inner and outer walls. The validity of conventional numerical simulation methods for seismic analysis of self-installing platforms should be verified through physical model tests. Therefore,

it is necessary to conduct shaking table model tests for self-installing platforms. However, since the structural components of the converter station are thin and the spatial structure is complex, the shaking table scaled model cannot achieve perfect similarity. Thus, to achieve the experimental objectives, it is necessary to explore appropriate simplifications for the shaking table model and verify their rationality.

2 Shaking Table Model Test Similarity Design of Offshore Converter Station

2.1 Prototype Structure of Offshore Converter Station

The typical cross-section of the self-installing platform for the offshore converter station in this experimental study is shown in Figure 1. The platform has a length of 121.6 m, a width of 84 m, and a depth of 21.5 m, supported by six shell-type pile legs with a diameter of 6 m and a wall thickness of 70 mm. The pile legs are 85 m above the seabed and are connected to fixed piles inserted into the seabed through grout connections at the bottom. The platform's lifting device uses hydraulic pins, with pin holes spaced 4 m apart along the axial direction of each pile leg, and four pin holes per layer. When the platform is fixed, each pile leg has eight pin holes that are inserted into pin shafts. The study focuses on the dynamic characteristics and seismic responses under seismic intensities of 7 and 8 degrees for water depths of 40 m and 48 m (the height of the platform varies with the water depth).

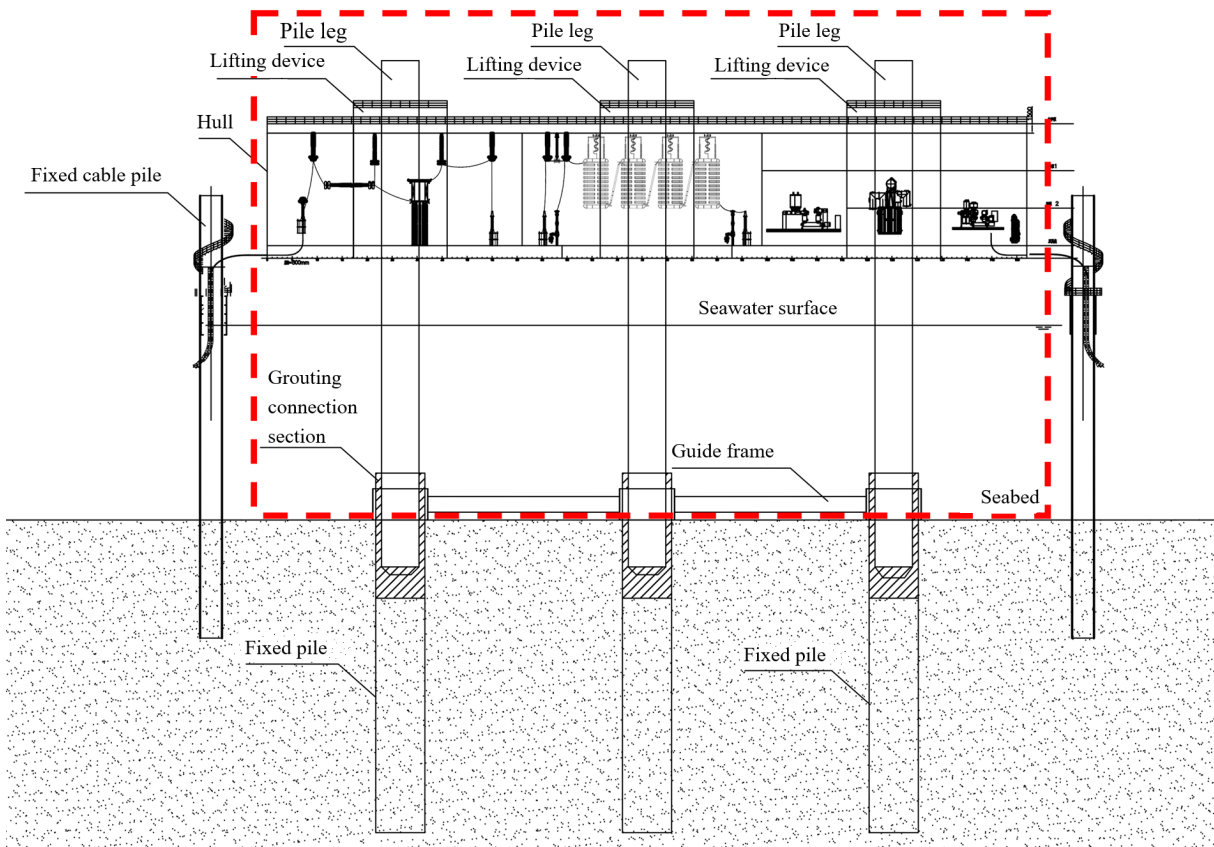


Figure 1. A cross-sectional diagram of offshore converter station and scope of test simulation

2.2 Main Experimental Equipment and Facilities

This experiment relies on the three-dimensional six-degree-of-freedom simulated earthquake underwater shaking table built at Hohai University. The detailed specifications are shown in Table 1. The pool size is $20 \times 30 \times 1.5$ m (length \times width \times height), and internal wave dissipation devices are arranged around the pool, which has been tested to provide good wave dissipation, meeting the requirements for offshore engineering pool wall wave dissipation.

2.3 Elastic Test Model Similarity Design

When the structure is within the small deformation, linear elastic range, the solid dynamic similarity conditions are as follows [21, 22]:

$$\frac{S_E S_\varepsilon}{S_\gamma S_l} = 1 \quad (1)$$

Table 1. Detailed specifications of the underwater shaking table for simulated earthquakes

Index Item	System Index (With Water)
Table surface size	Circular surface with a diameter of 5.75 m
Frequency range	0.1 ~ 80 Hz
Maximum load	≥ 30 tons (including water)
Overturning moment	60 ton-m
Eccentric distance	0.5 m
Maximum displacement	Horizontal ± 150 mm, Vertical ± 100 mm
Maximum speed	Horizontal ± 0.90 m/s, Vertical ± 0.95 m/s
Full load acceleration	Horizontal ± 1.55 g, Vertical ± 1.4 g

In the formula, S_E is the similarity ratio of the elastic modulus between the prototype and the model; S_ε is the similarity ratio of strain between the prototype and the model; S_γ is the similarity ratio of specific weight between the prototype and the model; S_l is the similarity ratio of length.

Based on the specifications in Table 1, considering the shaking table surface size and load, as well as the model size effects, the length similarity ratio of the model is determined to be 1:40, i.e., $S_l = 40$. Since water is still used to simulate the environment in the experiment, the model should satisfy $S_\rho = 1$. Moreover, since the model and the prototype are in the same gravitational field, this requires the model to satisfy $S_a = S_g = 1$, and the model's and prototype's unit weight should be the same. Additionally, in model tests involving interaction between structures and water, there are requirements for the test materials to have low elastic modulus, appropriate strength, impermeability, and stability. The prototype structure is made of steel, and acrylic and aluminum alloy are selected as the model materials for the pile legs and the platform body, respectively. The elastic modulus of the steel used in the prototype structure is 206 GPa, and the dynamic elastic modulus of the selected acrylic is 3.85 GPa. Thus, we have $S_E = 53.50$. According to Formula (1), we have $S_\varepsilon = 0.75$. Other similarity constants can be calculated using similarity relations as shown in Table 2.

Table 2. Model similarity constant (prototype/model)

Physical Quantity	Similarity Relationship	Similarity Constant	Remarks
Length l	S_l	40.00	
Density ρ	S_ρ	1.00	Weighting method
Acceleration a	$S_a = S_g$	1.00	
Unit weight γ	$S_\gamma = S_\rho S_g$	1.00	
Elastic modulus E	S_E	53.5	
Poisson's ratio μ	S_μ	1.00	
Strain ε	$S_\varepsilon = S_l S_\gamma S_E^{-1}$	0.75	
Stress σ	$S_\sigma = S_\gamma S_l$	40.00	
Displacement u	$S_u = S_\varepsilon S_l$	30	
Velocity v	$S_v = S_l S_t^{-1}$	7.31	
Stiffness k	$S_k = S_E S_l^4$	1.37×10^8	Pile leg bending stiffness equivalence
Time t	$S_t = S_l S_\rho^{1/2} S_E^{-1/2}$	5.47	
Frequency f	$S_f = S_t^{-1}$	0.18	

3 Offshore Converter Station Shaking Table Model Simplified Design

3.1 Model Simulation Range

Due to limitations such as geometric scale and water depth of the shaking table, the foundation cannot be simulated in the experimental model. The primary focus of this experimental model is the main structure and pile leg of the converter station. The selected simulation range is marked by a dashed line in Figure 1.

3.2 Dynamic Characteristics Equivalence of Foundation Pile-Soil Interaction

As shown in Figure 1, the offshore converter station platform's pile legs are connected to fixed piles through grout connections at the seabed. To accurately reflect the platform's dynamic characteristics and seismic response, it would be ideal to simulate the foundation as well. However, due to experimental constraints, the selected simulation range does not include the foundation. To account for the effect of the foundation, the dynamic characteristics

equivalence method is adopted. As shown in Figure 2, an overall finite element model of the structure and foundation is established for a water depth of 48 m (Model 1), and the natural frequency f_1 of the structure is calculated. Then, a model without the foundation and structure below the mudline (Model 2) is created. The position of the guide frame is adjusted through modal analysis until the natural frequency f_2 of the two models becomes approximately equal. The position of Model 2 when the frequencies are close is then used as the prototype for this experiment. The calculation results for the natural frequencies are shown in Table 3. When the guide frame position is raised by 17.5 m, the natural frequencies f_2 and f_1 differ by less than 0.01 Hz, indicating that the frequencies are nearly identical. This frequency difference is considered negligible, and the model corresponding to this adjusted position is used for the experimental simulation. After applying the length scale factor, the guide frame of the experimental model is raised by 437 mm compared to the original position.

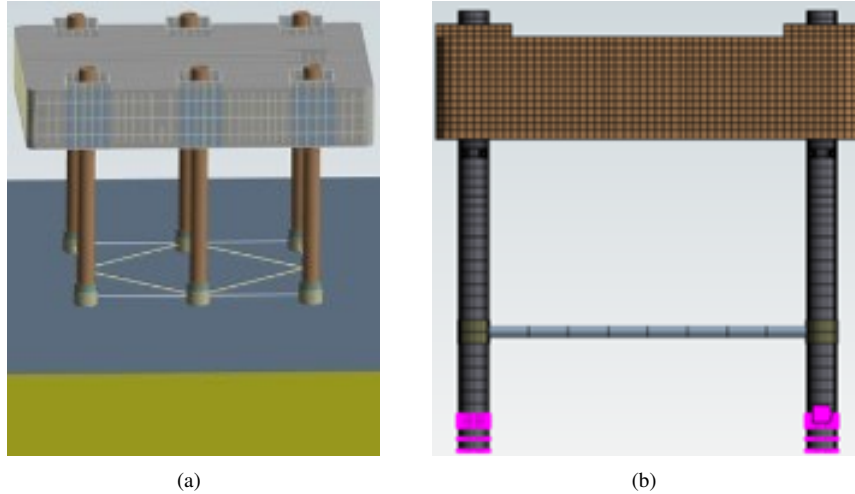


Figure 2. Equivalent finite element model of dynamic characteristics: (a) Model 1 (With Foundation); (b) Model 2 (Without Foundation, Guide Frame Raised by 17.5 m)

Table 3. Natural frequency of equivalent model of dynamic characteristics

Mode	Model 1	Model 2	Frequency Difference
1st Mode/Hz	0.5126	0.5212	-0.0086
2nd Mode/Hz	0.5212	0.5304	-0.0092
3rd Mode/Hz	0.6211	0.6300	-0.0089

3.3 Pile Leg Bending Stiffness Equivalence and Weighting Design

Since the prototype pile legs are made of steel pipes with relatively thin wall thickness, acrylic pipes are used as the model material. However, it is difficult to find acrylic pipes on the market that fully satisfy the geometric scaling of both wall thickness and diameter. Considering that the pile legs primarily undergo bending deformation under seismic conditions, the bending stiffness (EI) is used for equivalence (equivalence of the moment of inertia of the cross-section). The formula for the moment of inertia of a hollow circle cross-section is given by:

$$I_x = I_y = \frac{\pi}{64} (D^4 - d^4) \quad (2)$$

where, I_x and I_y are the moments of inertia about the X-axis and Y-axis, respectively; D is the outer diameter, and d is the inner diameter of the hollow circle. After collecting available acrylic pipe specifications from the market, as shown in Table 4, it was calculated that two types of acrylic pipes have moments of inertia that closely match those of geometrically scaled models.

Because the density of PMMA (acrylic) is lower than that of steel, lead blocks are used for weighting to make the PMMA tube's equivalent density match the required density ratio. The lead blocks are arranged in layers along the axis inside the pile legs, with four blocks per layer. To verify the rationality of the bending stiffness equivalence and weighting design of the model pile legs, dynamic characteristic tests are conducted for two types of pile legs, and the results are compared with the finite element simulation results of the prototype pile legs. As shown in Table 5, the

weighting significantly changes the dynamic characteristics of the model pile legs, and both types of pile legs align well with the fundamental frequency obtained through finite element analysis, proving that the bending stiffness equivalence and weighting design of the model pile legs are reasonable. To allow the test model to withstand greater external forces, the PMMA tube with a thicker wall (Spec 1) was ultimately selected as the material for the final simulated pile legs.

Table 4. Calculation of the moment of inertia for PMMA tubes of different specifications

Size Specifications	Outer Diameter D/mm	Inner Diameter d/mm	Wall Thickness/mm	Moment of Inertia/mm ⁴	Error/%
Perfect similarity	150	146.5	1.75	2239456	-
Spec 1	110	100	5	2278146	1.73
Spec 2	125	119	3	2140539	-4.42

Table 5. Comparison of dynamic characteristics test results and numerical simulation results for single pile leg models

Specification	Fundamental Frequency without Weighting (Hz)	Fundamental Frequency with Weighting (Hz)	Finite Element Prototype Frequency (Hz)	Converted Model Frequency (Hz)
Spec 1	8.30	4.39	0.839	4.58
Spec 2	9.28	4.39		

3.4 Platform Main Body Mass Equivalence

This experiment mainly investigates the overall structure's dynamic characteristics and dynamic response. The platform's local stiffness is significantly higher than that of the pile legs, so the platform body can be appropriately simplified. The goal is to ensure that the platform's mass, center of gravity, key equipment mass, and positions match the prototype structure. The stiffness similarity requirement for the platform body is relaxed but must still have enough stiffness. The elastic modulus of aluminum alloy is 71.7 GPa, much higher than that of PMMA, so the stiffness of aluminum alloy sheets of the same thickness is also significantly higher than that of PMMA sheets, which can meet the simplified requirements of mass similarity and adequate stiffness for the platform model, ensuring similar deformation in the model's pile legs. The specific simplifications are as follows: (1) For the platform body, aluminum alloy is selected as the model material. Since the density of aluminum alloy is less than steel, the plate thickness for each part of the model is adjusted to ensure mass similarity. (2) For the key equipment, iron blocks of similar mass are used to simulate the mass and position at the corresponding locations (see Figure 3).



Figure 3. Platform main body model processing: (a) Platform main body bottom plate, outer wall, and internal equipment weighting; (b) Platform internal bulkhead

3.5 Hydraulic Pin Simulation

For the experiment, holes are drilled at corresponding positions on the model pile legs, with a spacing of 200 mm. Each pile leg has 3 layers of 12 pin holes. As the water depth changes during the test, the height of the platform model also changes accordingly. For a water depth of 1 m, the first and second layers of pin holes in the pile legs are inserted, and for a water depth of 1.2 m, the second and third layers of pin holes are inserted. In the experiment, acrylic pin shafts are used to simulate hydraulic pin metal shafts, and foot sleeves are processed to replace the connection device between the platform body and pile legs. As shown in Figure 4 the pile legs are inserted into the foot sleeves, and acrylic pin shafts are inserted into the upper circular holes of the foot sleeves and the pin holes on the pile legs. A retaining plate is installed on the pin shaft to prevent it from falling off during the experiment. The bottom flange of the foot sleeve is bolted to the platform base for fixing.

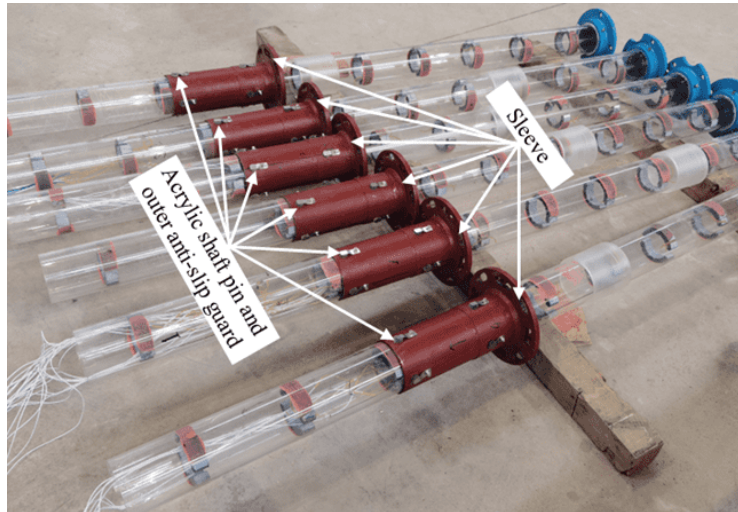


Figure 4. A cross-sectional diagram of offshore converter station and scope of test simulation

3.6 Pile Leg Water-facing Surface Equivalence

Since the acrylic tube diameter of 110 mm selected according to the bending stiffness principle does not satisfy the geometric similarity for the pile leg outer diameter, the water-facing surface needs to be enlarged to ensure that hydrodynamic pressure similarity is maintained. However, the impact of increasing the water-facing surface should have minimal effects on the model pile leg stiffness and mass. Extruded polystyrene (XPS) foam boards, which have both lightweight and certain stiffness properties, are selected as the material to increase the water-facing surface. The XPS foam boards need to be processed into semi-circular rings, with an outer diameter of 150 mm and an inner diameter of 110 mm. These two pieces of foam board are tightly bound to the model pile leg using zip ties.

3.7 Axial Stiffness Equivalence of the Guide Frame

The guide frame consists of a vertical guide tube, horizontal braces, and diagonal braces. The vertical guide tube is equivalently represented by bending stiffness, while the horizontal and diagonal braces mainly carry axial forces and are therefore modeled using PMMA tubes. The axial stiffness (EA) equivalence is selected based on available tube sizes while minimizing the effect of the weight of the horizontal and diagonal braces. The vertical sleeves, horizontal braces, and diagonal braces are connected using a special PMMA adhesive to ensure strong and reliable connections (see Table 6).

Table 6. Equivalent dimensions of axial stiffness of guide frame

Guide Frame Part	Fully Geometrically Similar Outer Diameter (mm)	Fully Geometrically Similar Wall Thickness (mm)	Equivalent Outer Diameter (mm)	Equivalent Wall Thickness (mm)
Horizontal braces	62.5	1.75	55	2
Diagonal braces	30	1	16	2

4 Converter Station Shaking Table Model Test Plan

4.1 Measurement Point Layout

4.1.1 Acceleration measurement points

In this experiment, three-dimensional accelerometers are used for the acceleration measurement points. The focus is on measuring points at the bottom of the pile legs, at the connection between the platform and pile legs, and on the hull. For convenience, the six pile legs of the model are numbered in a clockwise manner (the same applies later). The numbering of pile legs and the arrangement of acceleration measurement points are shown in Figure 5. Point A0 is located at the center of the table. Points A1 and A2 are at the bottom of pile legs 1 and 5, respectively. Points A3–A10 are located at the 8 corner points of the platform. Points A11–A16 are located on the tops of pile legs 1 to 6. This gives a total of 17 measurement points, with each accelerometer monitoring the X, Y, and Z directions, leading to a total of 51 data acquisition channels. The accelerometer data is used to acquire the dynamic characteristics of the model and the acceleration response under seismic wave excitation.

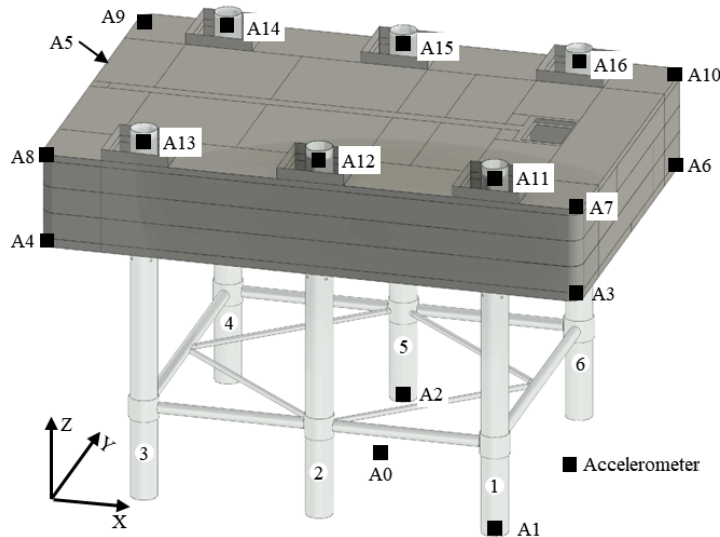


Figure 5. Acceleration measurement points layout diagram

4.1.2 Strain measurement points

Strain measurement is conducted to determine the stress state of the structure and assess its safety. The strain measurement points are arranged as shown in Figure 6. At the bottom of the pile legs, the strain measurement points are arranged as shown in Figure 6a. Pile legs 1 and 5 each have 4 three-axis strain gauges placed at a 45° angle, while the other pile legs have 4 vertical strain gauges at the bottom. At the pile leg pin holes, the measurement points are arranged as shown in Figure 6b. Pile leg 1 has strain gauges placed vertically on the inner walls of the first three layers of pin holes (12 strain gauges in total). Pile legs 2, 4, and 6 each have strain gauges placed on the first, second, and third layer inner walls of pin holes (12 strain gauges in total). At a water depth of 1 m, each pile leg will have the pins inserted into the first and second layers of pin holes. At a water depth of 1.2 m, as the platform height increases, the pins will be inserted into the second and third layers of pin holes. For each test, 56 data acquisition channels will be used.

4.1.3 Dynamic water pressure measurement points

To investigate the strength of the pile-leg-fluid coupling under seismic action, dynamic water pressure needs to be monitored. The layout of the dynamic water pressure measurement points is shown in Figure 7. Due to the symmetry of the model pile legs, dynamic water pressure is monitored on three pile legs (pile legs 1, 2, and 3). The lowest water depth for the experiment is 1m, so the dynamic water pressure sensors are placed at heights below 1m. To study the distribution of dynamic water pressure along the height of the pile legs, three sensors are placed at heights of 0 m, 0.45 m, and 0.9 m. As the structure will undergo reciprocating motion under seismic excitation, the following sensor arrangements are made: On pile leg 1, sensors DW1, DW2, and DW3 are placed at heights 0m, 0.45 m, and 0.9 m, respectively, along the X direction. On pile leg 2, sensors DW7, DW8, and DW9 are placed along the Y direction. On pile leg 3, sensors DW10, DW11, and DW12 are placed along the X direction, and sensors DW13, DW14, and DW15 are placed along the Y direction. A total of 15 dynamic water pressure sensors are used, with 15 data acquisition channels.

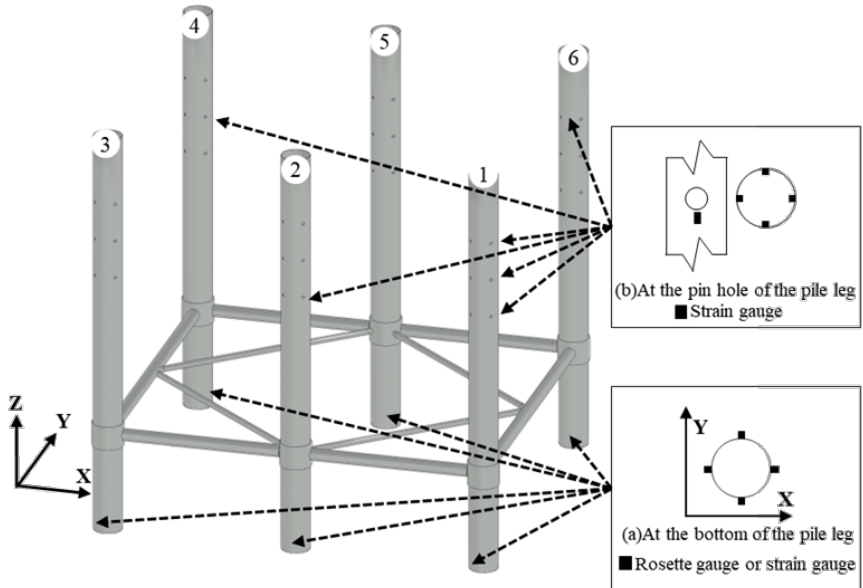


Figure 6. Schematic diagram of strain measurement point layout

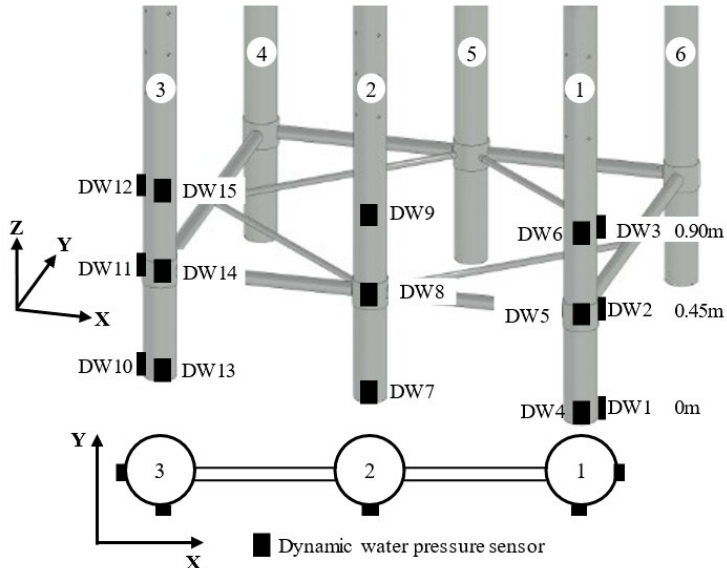


Figure 7. Schematic diagram of dynamic water pressure measurement point layout

4.2 Experimental Conditions

A total of three natural earthquake waves and one artificial wave are used for the experiment, with the artificial wave generated based on the response spectrum according to the seismic design specifications for water transport engineering (JTS146-2012). The experimental conditions are as follows: Water depths of 1.0 m and 1.2 m, with excitation levels corresponding to seismic fortification intensities of 7 and 8 degrees. The vertical excitation is scaled to 0.67 times the horizontal excitation. Specific experimental conditions are shown in Table 7. To study the effects of different water depths and platform heights on the dynamic characteristics and dynamic response of the converter station structure, two different water depths and platform installation heights are tested. The experiment is divided into three main phases: (1) Phase 1 (Water Depth 1 m): The platform base is fixed to the six supporting pile legs with four M30 bolts per leg. The water pool is filled to a depth of 1 m, and the shaking table tests are conducted according to conditions 1–11 in Table 7. After each condition is tested, the water is allowed to settle before moving to the next condition. (2) Phase 2 (Platform Lifting Phase).

Since the platform may be submerged at a water depth of 1.2 m, the self-lifting platform is raised to 1.45 m before conducting the 1.2 m water depth test. After completing all tests at 1m water depth, the water pool is emptied. The

platform is then lifted to 1.45 m using the lifting device, and two sets of pins are used to secure the platform and pile legs. (3) Phase 3 (Water Depth 1.2 m): After refilling the pool to a water depth of 1.2 m, the remaining conditions (12–22 in Table 7) are tested. The on-site experimental setup is shown in Figure 8.

Table 7. Test cases of the shaking table model

Test Case No.	Water Depth/ m	Seismic Excitation Wave	Direction	Peak Acceleration/ g	Test Case No.	Water Depth/ m	Seismic Excitation Wave	Direction	Peak Acceleration/ g
1	1.0	White noise El centro earthquake wave	XYZ	0.05	12	1.2	White noise El centro earthquake wave	XYZ	0.05
2	1.0	Artificial earthquake wave	XYZ	0.1/0.1/0.067	13	1.2	Artificial earthquake wave	XYZ	0.1/0.1/0.067
3	1.0	Wenchuan earthquake wave	XYZ	0.1/0.1/0.067	14	1.2	Wenchuan earthquake wave	XYZ	0.1/0.1/0.067
4	1.0	Great east Japan earthquake wave	XYZ	0.1/0.1/0.067	15	1.2	Great east Japan earthquake wave	XYZ	0.1/0.1/0.067
5	1.0	White noise El centro earthquake wave	XYZ	0.1/0.1/0.067	16	1.2	White noise El Centro earthquake wave	XYZ	0.1/0.1/0.067
6	1.0	Artificial earthquake wave	XYZ	0.2/0.2/0.133	17	1.2	Artificial earthquake wave	XYZ	0.2/0.2/0.133
7	1.0	Wenchuan earthquake wave	XYZ	0.2/0.2/0.133	18	1.2	Wenchuan earthquake wave	XYZ	0.2/0.2/0.133
8	1.0	Great east Japan earthquake wave	XYZ	0.2/0.2/0.133	19	1.2	Great east Japan earthquake wave	XYZ	0.2/0.2/0.133
9	1.0	White noise El centro earthquake wave	XYZ	0.2/0.2/0.133	20	1.2	White noise El Centro earthquake wave	XYZ	0.2/0.2/0.133
10	1.0	Artificial earthquake wave	XYZ	0.2/0.2/0.133	21	1.2	Artificial earthquake wave	XYZ	0.2/0.2/0.133
11	1.0	Wenchuan earthquake wave	XYZ	0.05	22	1.2	Wenchuan earthquake wave	XYZ	0.05



Figure 8. Offshore converter station self-installation platform shaking table model test

4.3 Dynamic Characteristics Validation

According to Table 7, Test Cases 1 and 12 both use white noise waves, which allow the dynamic characteristics of the model at water depths of 1 m and 1.2 m to be obtained. In addition, a finite element model of the prototype structure was established for modal analysis. Due to space limitations, only a comparison of the dynamic characteristics results

from the experiment are provided. The dynamic characteristics test results and the finite element modal analysis results are shown in Table 8, where the prototype fundamental frequency of the physical model test is converted to the prototype by using frequency similarity constants. The fundamental frequencies of the experimental model and numerical model follow the same trend with changes in water depth, and the frequency difference is less than 5%. This indicates that the dynamic characteristics of the experimental model are similar to those of the prototype, and the material selection and simplified design for the experimental model are reasonable. From the data in Table 8, it can be observed that both the physical model test and numerical simulation show a decreasing trend in the overall fundamental frequency as the water depth increases. This is mainly due to the added mass of the fluid on the structure caused by the fluid-structure interaction, and also because the overall stiffness of the structure decreases as the platform height increases.

Table 8. Comparison of the fundamental frequencies

Physical Model Test				Numerical Simulation Analysis		
Test water depth/m	Test model fundamental frequency/Hz	Similar prototype water depth/m	Prototype fundamental frequency/Hz	Prototype water depth/m	Prototype fundamental frequency/Hz	Relative error
1.0	3.42	40	0.6252	40	0.5982	4.3%
1.2	2.69	48	0.4918	48	0.4996	1.6%

5 Conclusion

The shaking table model test of the offshore self-installing converter station platform not only allows for the prediction of the earthquake response of the prototype structure but also guides the seismic design of actual engineering projects. It also validates the effectiveness of numerical simulation results. However, due to the complexity of the prototype structure and the impossibility of achieving full similarity after geometric scaling, it is necessary and important to simplify the model design to achieve the test objectives. This paper mainly addressed the issue of designing an elastic similarity model for a small-scale offshore converter station shaking table, covering multiple aspects such as similarity design, material selection, model simplification, measurement point layout, and test case design. The comparison of the dynamic characteristics test results with the finite element modal analysis results verified that the experimental model design is reasonable, and it is expected to provide a reference for shaking table tests of offshore platforms.

Data Availability

The data used to support the findings of this study are available from the corresponding author upon request.

Conflicts of Interest

The authors declare that they have no conflicts of interest.

References

- [1] S. J. Cao, J. L. Wang, X. Z. Wu, and W. Z. Bai, “Review on offshore wind power transmission technologies,” *Electrotech. Electr.*, vol. 2020, no. 9, pp. 66–69, 2020.
- [2] X. J. Jin, X. Z. Li, and D. Li, *Large Platform Floatover Method Research and Practice*. Beijing, China: Science Press, 2017.
- [3] T. Y. Li, S. F. Liu, Y. Y. Zhang, R. Li, and X. X. Xu, “Analysis and discussion on the construction technology of offshore platform jackets,” *Petro Chem. Equip.*, vol. 27, no. 9, pp. 157–160, 2024.
- [4] P. Wei, H. Zhang, S. L. Xue, N. Li, and Y. Zhou, “Application of modern shipbuilding mode in the construction of jack-up drilling platforms,” *Mech. Eng.*, vol. 2016, no. 5, pp. 194–196, 2016.
- [5] H. Y. Wang, “Tempo-spatial distribution of marine seismicity and its tectonic environment analysis of China offshore seas,” Master thesis, Nanjing: Nanjing University, 2014.
- [6] W. D. Shao, J. L. Hou, L. Q. Wang, C. J. Yu, D. F. Fu, and H. Cao, “Analysis of ductility-earthquake resistance for jacket platforms taking account of the nonlinearity,” *China Offshore Oil Gas*, vol. 28, no. 4, pp. 125–131, 2016.
- [7] Y. H. Jin, P. L. Yan, E. D. Guo, H. L. Wu, R. Z. He, and X. N. Wang, “Dynamic response analysis of offshore jacket platform under the coupling action of the earthquake and typhon,” *Technol. Earthq. Disaster Prev.*, vol. 17, no. 1, pp. 132–142, 2022.

- [8] F. F. Li, "Structural dynamic response analysis of offshore platform jacket under extreme conditions of impact and earthquake," Master thesis, Wuhan: Huazhong University of Science and Technology (HUST), 2020.
- [9] M. N. Wu, J. J. Wu, X. Y. Li, and M. Y. Zhang, "Seismic dynamic response analysis of offshore jacket platforms based on the time history analysis method," *Ship Eng.*, vol. 46, no. 2, pp. 115–123, 2024.
- [10] Z. M. Ghazi, I. S. Abbood, and F. Hejazi, "Dynamic evaluation of jack-up platform structure under wave, wind, earthquake and tsunami loads," *J. Ocean Eng. Sci.*, vol. 7, no. 1, pp. 41–57, 2022. <https://doi.org/10.1016/j.joes.2021.04.005>
- [11] Z. Sun, Y. Yu, H. Wang, S. Huang, and J. Chen, "Dynamic response analysis of offshore converter station based on vector form intrinsic finite element (VFIFE) method," *J. Mar. Sci. Eng.*, vol. 10, no. 6, p. 749, 2022. <https://doi.org/10.3390/jmse10060749>
- [12] S. X. Zhao, C. W. Bi, and Z. Z. Sun, "Engineering analysis of the dynamic characteristics of an electrical jacket platform of an offshore wind farm under seismic loads," *Appl. Ocean Res.*, vol. 112, p. 102692, 2021. <https://doi.org/10.1016/j.apor.2021.102692>
- [13] W. Xie, Q. Zhang, B. Gao, G. Ye, W. Zhu, and Y. Yang, "Shaking table tests for seismic response of jack-up platform with pile leg-mat foundation on sandy seabed," *Ocean Eng.*, vol. 309, p. 118564, 2024. <https://doi.org/10.1016/j.oceaneng.2024.118564>
- [14] Y. Chai, Q. Zhang, B. Yan, W. Zhu, and G. Ye, "Dynamic response of hybrid foundation for jack-up platform on sandy seabed under horizontal cyclic loading," *Soil Dyn. Earthq. Eng.*, vol. 194, p. 109336, 2025. <https://doi.org/10.1016/j.soildyn.2025.109336>
- [15] F. Liu, "PTMD vibration control method and experimental study on jack-up offshore platforms," Master thesis, China University of Petroleum (East China), 2021.
- [16] Y. K. Lou, X. Li, W. H. Wang, J. J. Zuo, and Y. Zhong, "Dynamic model test of offshore substation platform under earthquakes," *Acta Energ. Sol. Sin.*, vol. 40, no. 1, pp. 277–284, 2019.
- [17] R. He and L. Pan, "Seismic responses and vibration control of offshore wind turbines considering hydrodynamic effects based on underwater shaking table tests," *Earthq. Eng. Struct. Dyn.*, vol. 53, no. 2, pp. 545–572, 2024. <https://doi.org/10.1002/eqe.4035>
- [18] Y. Y. Ko and Y. T. Li, "Response of a scale-model pile group for a jacket foundation of an offshore wind turbine in liquefiable ground during shaking table tests," *Earthq. Eng. Struct. Dyn.*, vol. 49, no. 15, pp. 1682–1701, 2020. <https://doi.org/10.1002/eqe.3323>
- [19] S. Huang, D. Yu, W. Bai, X. Guo, and J. Dai, "Experimental and numerical analysis of seismic performance of jacket platforms subjected to onshore and offshore earthquakes," *Eng. Struct.*, vol. 311, p. 118177, 2024. <https://doi.org/10.1016/j.engstruct.2024.118177>
- [20] S. Liu, H. Li, J. Zhang, S. Yang, and T. Zhang, "Shaking table test and numerical simulation of jacket offshore platform considering soil-water-structure interaction," *Ocean Eng.*, vol. 313, p. 119542, 2024. <https://doi.org/10.1016/j.oceaneng.2024.119542>
- [21] D. Q. Zuo, *Theory and Methods of Model Testing*. Beijing: Water Resources and Electric Power Press, 1984.
- [22] S. Y. Xia, C. F. Zhang, and M. Q. Zhang, "Discussions on similarity conditions for dynamic structural models—with some comments on 'Research on similarity laws for arch dam vibration models,'" *J. East China Inst. Water Conserv.*, vol. 1980, no. 1, pp. 59–72, 1980.